ASME Turbo Expo 2020: Turbomachinery Technical Conference and Exposition,
September 21–25, 2020, Virtual, Online, GT2020-15107
DOI:10.1115/GT2020-15107

INTEGRATED SYSTEMS SIMULATION FOR ASSESSING FUEL THERMAL MANAGEMENT CAPABILITIES FOR HYBRID-ELECTRIC ROTORCRAFT

Ioannis Roumeliotis, Lorenzo Castro
Cranfield University, UK
i.roumeliotis@cranfield.ac.uk, nerolcasven94@gmail.com

Soheil Jafari, Vassilios Pachidis
Cranfield University, UK
S.Jafari@cranfield.ac.uk, v.pachidis@cranfield.ac.uk

Louis De Riberolles, Olivier Broca, Deniz Unlu
Siemens Industry Software, France
olivier.broca@siemens.com,Louis.deriberolles@siemens.com,
deniz.unlu@siemens.com

ABSTRACT

Future aircraft and rotorcraft propulsion systems should be able to meet ambitious targets and severe limitations set by governments and organizations. These targets cannot be achieved through marginal improvements in turbine technology or vehicle design. Hybrid-electric propulsion is being widely considered as a revolutionary concept to further improve the environmental impact of air travel. One of the most important challenges and barriers in the development phase of hybrid-electric propulsion systems is the Thermal Management System (TMS) design, sizing and optimization for addressing the increased thermal loads due to the electric power train.

The aim of this paper is to establish an integrated simulation framework including the vehicle, the propulsion system and the fuel-oil system (FOS) for assessing the cooling capability of the FOS for the more electric era of rotorcrafts. The framework consists of a helicopter model, propulsion system models, both conventional and hybrid-electric, and a FOS model. The test case is a twin-engine medium (TEM) helicopter flying a representative Passenger Air Transport (PAT) mission.

The conventional power plant heat loads are calculated and the cooling capacity of the FOS is quantified for different operating conditions. Having established the baseline, three different Power Management Strategies (PMS) are considered and the integrated simulation framework is utilized for evaluating FOS temperatures. The results highlight the limitations of existing rotorcraft FOS to cope with the high values of thermal loads associated with hybridization for the cases examined. Hence, new ideas and embodiments should be identified and assessed. The case of exploiting the fuel tank as a heat sink is investigated and the results indicate that recirculating fuel to the fuel tank can enhance the cooling capacity of conventional FOS.

INTRODUCTION

The global helicopter market expects an increase of 3.4% during the 2017-2023 period [1]. The new generation of helicopter engines are increasingly complex with higher requirements for mobility, safety, and stealth resulting in hotter fluids, higher components temperature, and higher heat generation, which means critical thermal management issues. Moreover, the development of new technologies should take regulations for environmental considerations into account like pollutant emissions and fuel consumption [2]. Electrification is a revolutionary concept in this regard. As discussed by Danis et al [3], Voskuijl et al. [4] and Roumeliotis et al. [5] transitioning to hybrid-electric propulsion can benefit rotary-wing aircraft.

Hybrid electric configurations for rotorcraft propulsion are expected to have high needs for systems cooling due to the high heat dissipation of the electric power train components [6]. In this context, the increased electrification of various subsystems is expected to increase the importance of thermal management making the full exploitation of available thermal sinks a necessity. During the last two decades, several research studies have been published on thermal management systems for the new and next generation of civil aero-engines [7], more electric aircraft (MEA) program [8], energy optimization aircraft (EOA) program [9], and integrated thermal management systems design for conventional rotorcrafts [10]. However, the thermal management requirements for the hybrid electric concepts have not been explored, while little attention has been drawn on rotorcraft hybrid electric configurations.

Fuel is the main heat sink for rotorcrafts so it is significant to assess the cooling capability of the existing fuel system for quantifying future needs and identify methods for fully exploiting it as a heat sink. Traditionally, the air vehicle, propulsion and power systems and FOS are analyzed at a subsystem level with little consideration on systems integration, thus the systems interaction and the overall performance are not fully assessed as discussed by Wolff [11] and Walters et al. [12]. For enabling hybridization, it is important to exploit the full potential for heat dissipation in system level, taking into consideration sub-systems interactions, transients and identifying alternative heat sinks.

The aim of this paper is to assess the cooling capacity of conventional rotorcraft fuel system for a whole mission and identify the system capability to act as a heat sink for hybrid configurations. For this purpose, an integrated model for thermal management system simulation is developed in Simcenter Amesim [13]. The integrated model includes the helicopter model, the propulsion system model (conventional and hybrid) including its heat loads (mechanical and electrical) and the fuel and an oil system model.

The integrated model is used to assess the cooling capability of a conventional FOS for a TEM helicopter for a PAT mission and different take off weights (TOW). For identifying limiting factors, a standard and a hot day are considered. For enhancing the cooling capability of the FOS, fuel tank recirculation is applied and the system enhanced cooling capacity is quantified. Following, a parallel hybrid-electric propulsion system is simulated for providing the electrical heat loads for assessing the capability of these two FOS configurations to perform thermal management. Three different power management strategies are considered and the capabilities and limitations of the FOS to act as an integrated thermal management system for rotorcraft hybridization are recognized and discussed.

INTEGRATED THERMAL MANAGEMENT SYSTEM

For assessing the heat and energy management of the whole helicopter, a vehicle level integrated thermal management system model is developed and its sub-systems are described herein. The general framework is depicted in Figure 1.

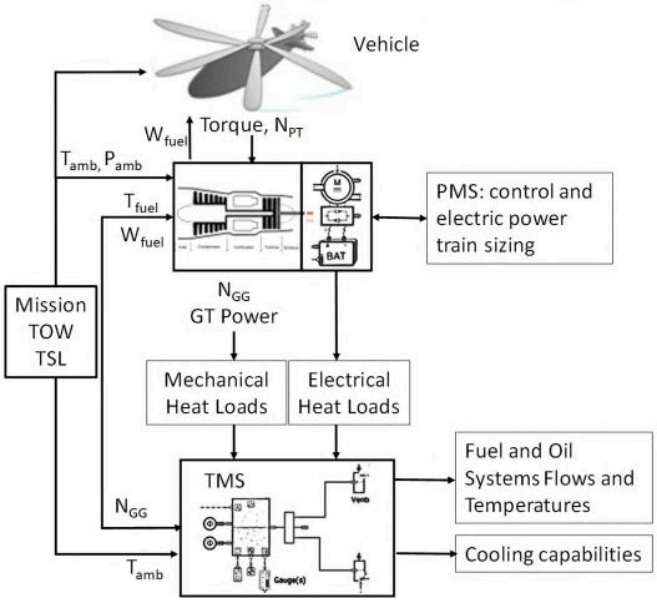

Figure 1: Integrated Thermal Management System Model

The helicopter model provides the boundary conditions (Torque and rotor rotational speed, which is translated to power demand and power turbine rotational speed - N_{PT}) to the propulsion system, according to TOW and mission parameters. The HEP propulsion system is sized according to the PMS; while the conventional propulsion system utilize the baseline gas turbine. A control scheme is used for defining the fuel flow based on vehicle power demand and PMS. The injected fuel flow (W_{fuel}) is provided to the helicopter model to update the system weight and to the gas turbine engine for setting its operating point. Then the gas turbine model provides the gas generator rotational speed (N_{GG}) and power (GT Power) for calculating the engine mechanical heat loads, while the electric power train components provide the heat loads. The gas generator rotational speed is provided to the FOS system for calculating the oil and the total recirculating fuel flows. Then with the fluid flows (recirculating fuel, engine delivered fuel (injected), oil) and the heat loads and ambient conditions the fuel and oil line temperatures are calculated. The fuel temperature (T_{fuel}) is fed back to the gas turbine model. The ambient temperature is calculated based on sea level temperature (TSL) and the altitude. The tank temperatures are assumed equal to the ambient temperature prior to taking off.

Helicopter Modelling

A UH-60 helicopter performance model is used herein for simulating the vehicle, providing torque and power requirements along a designated mission scenario. The main rotor model is based on a blade-element-type discretization, comprising a steady and linear inflow model [14], coupled with a steady, non-linear airfoil aerodynamic representation. For the special case of hovering flight, a combined blade element momentum theory approach is employed for the evaluation of axisymmetric rotor inflow as discussed in [15]. Tail rotor power is estimated as a fraction of main rotor power based on the semi-empirical relation provided in [15]. Fuselage aerodynamic forces and moments are calculated based on look-up tables retrieved from [16]. In Figure 2 the comparison of the predicted main rotor power coefficient against published flight test data for a range of cruise advance ratios is presented for a weight coefficient Cw=0.0065 [17]. Very good agreement is observed between simulated and measured performance data.

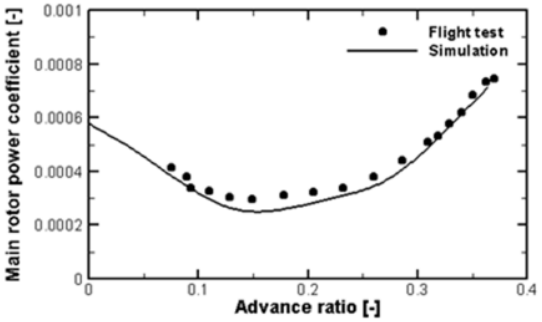

Figure 2: Main rotor power requirement for a range of advance ratios at Cw=0.0065 (-): comparison with flight test data retrieved from [17].

The helicopter model provides the propulsive power demand as a function of mission and helicopter weight, which acts as boundary condition for the propulsion control system.

Propulsion System

Two propulsion system models have been developed herein, the conventional gas turbine based and a parallel hybrid-electric (HEP) gas turbine based. The gas turbine conventional configuration acts as the baseline. The thermal – electric power split for the HEP system depends on the Power Management Strategy (PMS) applied. A basic control system is in place for the propulsion system, for both configurations, using the fuel flow as the gas turbine setting parameter for matching the power demand, which depends on the PMS, and the maximum continuous rating (MCR) turbine entry temperature as a limiter. The fuel consumption is fed to the helicopter model for updating the vehicle weight and consequently the propulsive power for each operating point.

Gas Turbine

The gas turbine engine model is based on the T700-GE-700, a turboshaft engine broadly used in Twin Engine Medium (TEM) helicopters. A model capable to represent with very good accuracy the steady state and transient operation of the engine has been developed and validated against available experimental data as presented by the authors in [5]. The model is capable of simulating the whole engine operating envelope with very good accuracy, as seen in Figure 3**.**

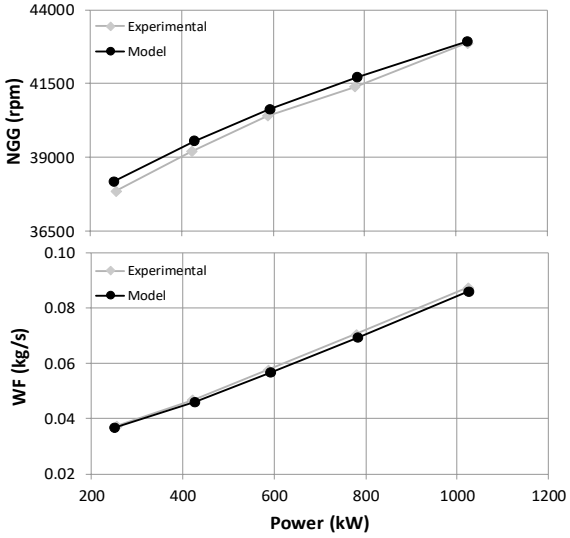

Figure 3: Gas turbine performance data, experimental values from [28]

Hybrid Propulsion System

A parallel hybrid propulsion model has been considered herein for each of the power sources of the helicopter. The model is built in Simcenter Amesim using components from the "Aircraft Electrics" and "Electric Motor and Drives" libraries ([29], [30]) in conjunction with the gas turbine engine model and is depicted in Figure 4.

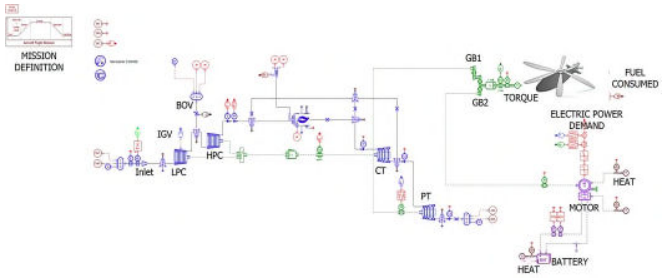

Figure 4: Gas Turbine based HEP parallel configuration model architecture

The motor is simulated using a functional model of an electric drive system (machine, inverter, sensor and control unit) for simplicity. The motor part load efficiency is calculated applying the procedure reported in [31]. The maximum efficiency considered is 0.94, according to [32]. For the batteries, the equivalent circuit model of battery pack available in Simcenter Amesim is used since it may provide the heat released during charges and discharges. The battery sizing is done according to [34] and [35] using nominal energy, power and voltage requirements utilizing a database of curves, such as the ones depicted in Figure 5. This process is performed by the software sizing tool. The ohmic resistance is defined allowing the ohmic resistance losses calculation.

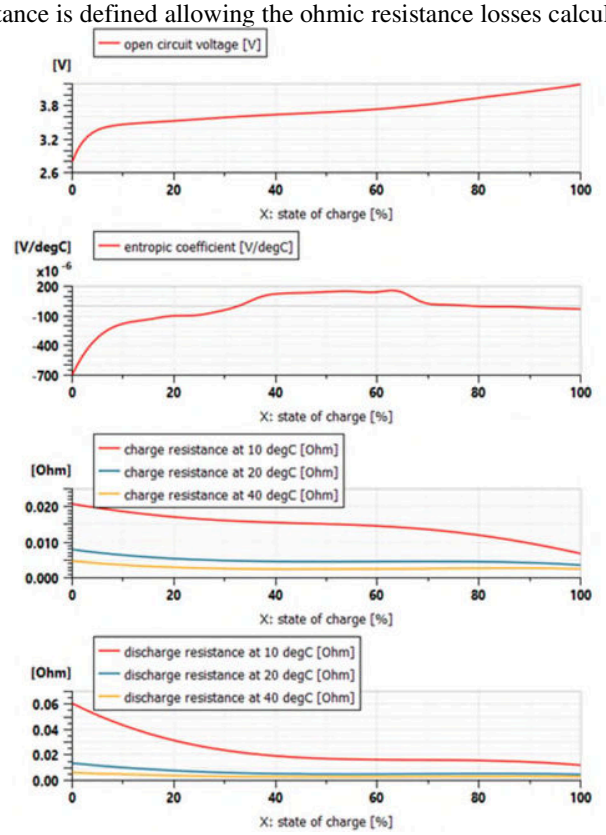

Figure 5: Battery scaled performance parameters for a nominal power of 1200kW, energy 150kWh and 3000V [13]

Three PMS cases are considered herein, one which is considered the worst case with respect to thermal loads, and two for highlighting hybridization effect. The PMS and the electric power train nominal data are discussed in the test cases section. The electric power train is sized according to the PMS selected and the relevant power and energy requirements.

Engine Heat Loads

Two gas turbine related heat sources are considered herein, the accessory gearbox (AGB) and the engine shaft bearings. The AGB allows extracting part of the mechanical power from the turbine transmitting it to "accessory" elements such as pumps and valves. As a mechanical transmission element, lubrication is needed to ensure satisfactory performance; hence oil flow will pass through it absorbing part of the heat generated. The same condition is applied to the engine shaft bearings. The rotational speeds and the power are provided by the engine model.

Accessory Gearbox Heat Loss Calculation

The transmitted power in the AGB can be lost through dissipation by gear teeth due to friction and by spin power losses accounted by surrounding environment. These heat loss mechanisms can be divided into no-load dependent losses (viscous) caused by gears, seals and bearings, and load-dependent (friction-induced) losses caused by gears and bearings.

No-load dependent losses mainly consist of windage and churning power losses. Churning loss occurs when the bearing or gear churn through the lubricant. Windage losses occur on rotating gears as frictional resistance due to the surrounding air. These losses occur in rotating mechanical components even without torque transmission and are related to density, viscosity of oil, immersion depth of the components on a sump, and the internal design of gearbox casing. For rolling bearings, no-load losses mainly depend on the size and bearing arrangement, immersion depth, and lubricant viscosity.

Load-dependent power losses occur between gear teeth during power transmission. They are mainly depending on friction coefficient, transmitted power, and sliding velocity in the contact area between teeth ([18], [19]). In addition, friction losses are the main source of gearbox power loss when transmitting high torque. However, the friction due to viscous forces of the lubricant must be considered when low torque is transmitted as well in order to estimate the power loss correctly.

Considering the above-mentioned descriptions, load dependent losses occur in gears and bearings while no-load dependent losses occur in gears, bearings, and seals. Therefore, five main heat loss mechanisms should be considered in the AGB as shown in Figure 6.

Figure 6: AGB heat loss mechanisms

In 2011, Changenet and Velex [20] measured the no-load dependent losses for high speed meshed gears with and without lubricant. Windage loss was measured without lubricant and deducted from the total losses. The gears churning loss was obtained applying thermal balance and eq. (1) has been deducted based on a series of experiments utilizing dimensional analysis.

The sliding loss is one of the most important sources of power losses in meshed gears, when speed is not too high. Buckingham ([21], [22]) proposed the first theoretical method to calculate the gear mesh efficiency, in 1949, by considering average friction coefficient along the contact line. Later, in 1958 Ohlendorf [23], proposed eq. (2) that account power loss for meshing gears. This formula is still widely used in the literature to calculate the gear mesh loss in gearboxes.

The bearings churning loss is calculated by utilizing the Palmgren model [24] shown in eq. (3).

The power losses due to bearings are directly proportional to the friction torque and rotational speed, according to eq. (4), [19]. An enormous number of measurements done by Freudenberg Simrit GmbH & Co. ([25], [26]) has been used to calculate seals friction losses. It was deducted that the seal friction torque increases with speed and seal diameter, deriving eq. (5) for predicting the power loss due to seal, however, the influence of oil viscosity is not considered in the formula.The equations for calculation these loss mechanisms are listed in **Table** 1. By applying eq. (1) to (5), the total heat load generated by the AGB is calculated via eq. (6).

Table 1: Physics-based equations for AGB heat loss calculation

Heat Loss Mechanism	**Formula**	
Gears Churning Loss	$PL_{G0} = \frac{1}{2} \cdot \rho \cdot \boldsymbol{\Omega^3} \cdot A_i \cdot R^3 \cdot C_m$	(1)
Meshing Gears Loss	$PL_G = P_{in} \cdot \mu_m \cdot H_v$	(2)
Bearings Churning Loss	$PL_{B0} = \Omega \cdot \left(f_0 \cdot 10^{-7} \cdot (n \cdot \mu_{oil})^{2/3} \cdot {d_m}^3\right) \cdot 10^{-3}$	(3)
Bearings Friction Loss	$PL_B = \frac{\pi}{30} \cdot n \cdot \left(\sqrt{F_R^2 + F_A^2} \cdot f_1 \cdot d_m\right)$	(4)
Seals Churning Loss	$P_{SO} = 7.69 \times 10^{-6} \cdot {d_i}^2 \cdot n$	(5)
Total Heat Loss	$PL = PL_{G0} + PL_G + PL_{B0} + PL_B + PL_{S0}$	(6)

Where:
P: power losses [kW]
ρ: lubricant density [kg/m^3]

Ω: AGB shaft rotational speed [rad/s]
A_i: immersion surface area [m^2]
$R = \frac{D}{2}$: the pitch radius [m]
C_m: flow regime coefficient [-]
μ_m: mean friction coefficient along the path of the contact [-]
H_v: gear loss factor [-]
P_{in} : power input [kW]
f_0: bearing coefficients of loss [-]
μ_{oil}: dynamic viscosity [kg. m. s^{-1}]
n: bearing rotational speed [rpm]
d_m: mean diameter of AGB shaft [m]
$F_R + F_A$: the summation of radial and axial load applied [N]
f_1 : the bearings friction coefficient [-]
d_i: the shaft diameter [m]

The Pitch diameter is 55 mm, the AGB shaft diameter 50 mm, the gear loss factor 0.25, f_0 and f_1 values are 0.0012 and 0.0018 respectively.

Bearings Heat Loss Calculation

Almost all friction loss (sum of rolling, sliding, and lubricant friction) in a bearing is transformed into heat within the bearing itself and is the main cause of the bearing oil temperature rise. The amount of thermal generation caused by friction moment can be calculated by eq. (7) [36]:

$$Q_R = 0.105 \times 10^{-6} M\, n \qquad (7)$$

where,

Q_R : Thermal value, kW

M : Friction moment, N・mm

n : Rotational speed, min-1

The friction moment is calculated by the method described in detail in [37].

Fuel Oil System

A fuel oil system that can be utilized with the baseline gas turbine is pre-designed based on publicly available data. A model of a variation of the baseline FOS utilizing tank fuel recirculation has been developed as well.

Baseline Fuel Oil System

The schematic of the baseline FOS is depicted in Figure 7.

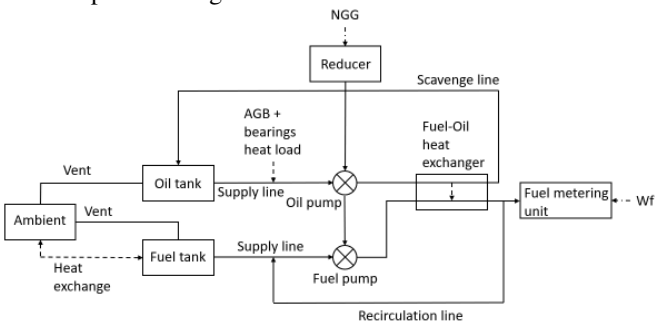

Figure 7: Baseline FOS schematic

The fuel system model is composed of a tank, supply and recirculation lines, a pump, the fuel-oil heat exchanger and the fuel metering unit. The lubrication system model is composed of a tank; supply and scavenge lines; heat sources representing the heat generated by the engine bearings and AGB; a pump; and the oil-fuel heat exchanger.

The fuel tank model considers the 3D geometry of the tank. It computes the remaining fuel quantity, its level, the fuel and ullage temperatures and pressures. A single 1.44 m^3 fuel tank has been assumed. As the tank is in the lower part of the vehicle, it is in contact with the helicopter skin. The radiative and convective heat exchanges between the atmosphere and the skin and then the tank are computed considering the rotorcraft altitude and speed, and the ambient temperature. Fuel is extracted from the tank through the supply line while the tank vent is connected to the atmosphere.

The pipes hydraulic area sizing is done by assuming a maximum fuel mass flow of 0.225 kg/s, including the recirculation, and of 0.15 kg/s in the injectors. The fuel flow maximum velocity is assumed 1 m/s [38]. The fuel pumps are assumed to pump a fuel flow proportional to the gas generator corrected rotational speed, which is provided by the gas turbine model. A simple "positive fixed-displacement pump has been selected and scaled versus fuel flow and maximum continuous rotational speed (0.225kg/s, 44700rpm), according to eq. (8). The maximum rotational speed for the fuel pump is set to 10000 rpm and through this value and the maximum mass flow, the volumetric flow is calculated.

$$Q\left[\frac{lt}{min}\right] = displacement\left[\frac{cc}{rev}\right] \cdot n[rpm] \qquad (8)$$

The fuel flow injected in the combustion chamber is derived by the propulsion system control scheme. The remaining fuel flow is recirculated through the recirculation line to the pump inlet.

The oil tank is a cuboid of 0.08m^3 and no heat exchange with the atmosphere is considered. The pipes hydraulic area sizing is done in a similar way as done for the fuel system. Heat loads from the accessory gearbox and bearings are applied to the oil. Those loads are variable and depend on the mission profile, as discussed. The oil pump produces flow rate proportional to the gas generator corrected rotational speed and is sized in a similar way as the fuel pump.

The fuel-oil heat exchanger is sized following the method discussed by Shawabkeh [39]. It uses both the NTU (Number of Transfer Units) and the LMTD (Log Mean Temperature Difference) methods and involves an interpolation process to find out the geometrical values and the heat exchanged. The fuel heater/oil cooler is a tube and shell design which is mounted adjacent to the fuel boost pump, where oil and fuel enter on the same end through face-ports in the gearbox. A baffled-flow, multi-pass design is used in order to minimise the pressure drop while obtaining maximum effectiveness. The fuel will flow through the tubes, while the oil flows over the shell.

The procedure is starting with assuming tube diameter, tube length, fouling factor, and material of construction for the tubes. Then, by utilizing the heat duty equation, the LMTD is calculated and then the temperature correction factor is derived based on the heat exchanger configuration. The mean temperature difference is computed using the temperature correction factor and the LMTD. After that, the provisional area is evaluated assuming the overall heat transfer coefficient. Then, the other geometrical parameters of the heat exchanger including number of tubes, bundle diameter, tube outside diameter, shell diameter, and baffle spacing can be derived. The final step is to calculate the shell-side mass velocity, Reynolds number, Prandtl number, and heat transfer equations to check the validity of the initial guesses. If the procedure does not converge, all steps are repeated until a set of compatible design values is achieved. The heat exchanged at the design point is 12kW with an LMTD of 24.66K, assuming an overall heat transfer coefficient of 150W/m^{2}ºC

Fuel Recirculating at the Tank

In order to increase the FOS cooling capability without drastic changes of the configuration, a model applying fuel tank recirculation is developed. The heated fuel instead of returning prior to the HP pump returns to the fuel tank, as seen in Figure 8.

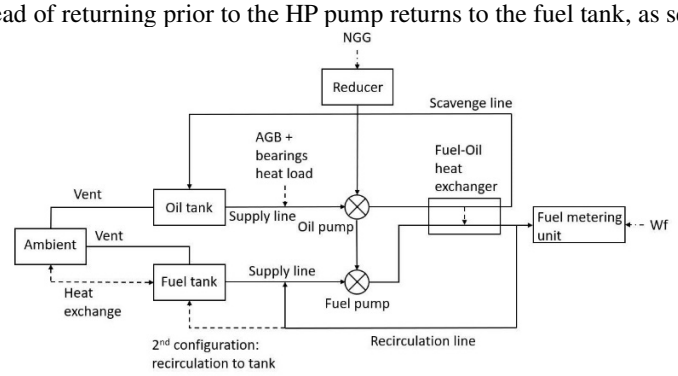

Figure 8: Tank recirculating FOS

FUEL OIL SYSTEM ASSESSMENT

In order to assess the baseline FOS capability to act as a heat sink for a hybrid configuration, firstly the baseline configuration is simulated for different TOW values and for a standard and a hot day. The cooling capacity of the system is quantified. Then the configuration utilizing fuel tank recirculation, that may allow higher cooling capability, is simulated and assessed. Following, three different PMS for the hybrid propulsion system are simulated and assessed in terms of overall system thermal management capability. The hybrid propulsion system is sized based on the PMS. The integrated thermal management and propulsion system model used for the configurations assessment as developed in Simcenter Amesim is presented in Figure 9. The limit temperatures considered herein for assessing the FOS has been suggested by Streifinger [40] and are summarized in Table 2.

Table 2: Working fluid temperature limits [40]

Rotorcraft Parameters	Value

Maximum fuel temperature burner in (steady)	130 ºC
Maximum fuel temperature burner in (transient)	140 ºC
Minimum fuel temperature boost pump inlet	-40 ºC
Maximum fuel temperature boost pump inlet	60 ºC
Maximum scavenge out oil temperature (steady)	165 ºC
Maximum scavenge out oil temperature (transient)	180 ºC
Maximum oil cooler out temperature (steady)	110 ºC
Maximum oil cooler out temperature (transient)	125 ºC

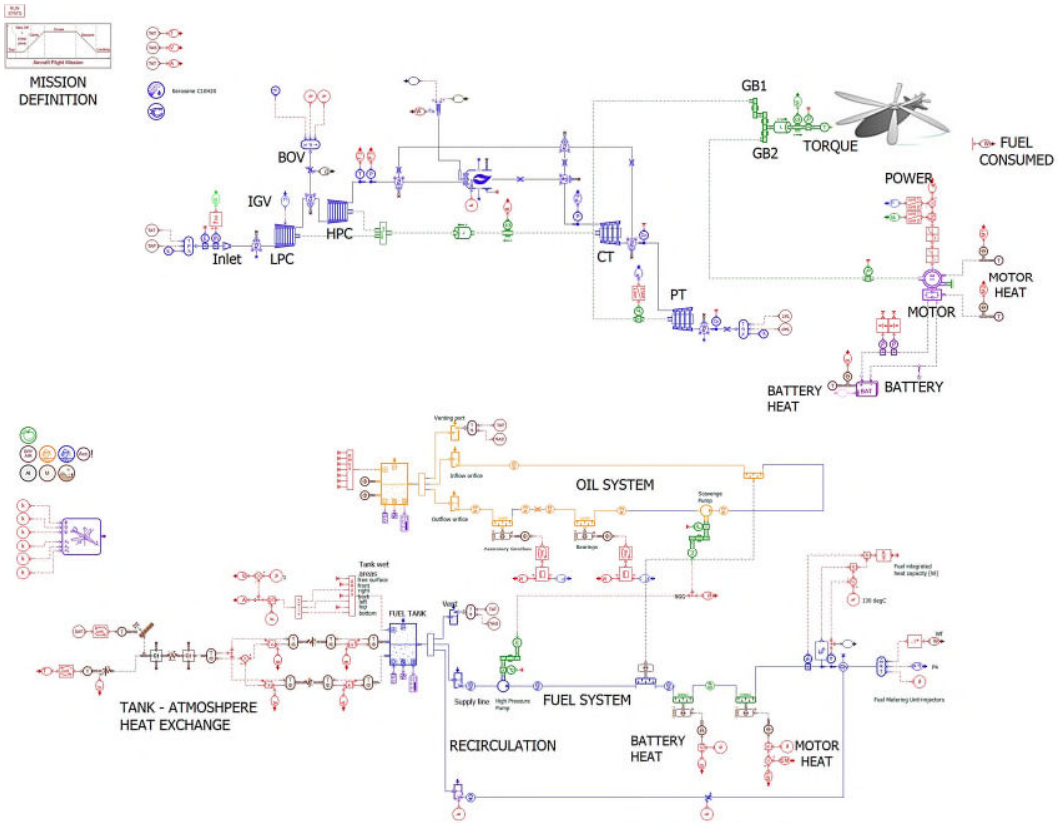

Figure 9: Integrated Fuel – Oil and Propulsion System Model (HEP & Tank Recirculation)

Test Case Mission

A Passenger Air Transport (PAT) scenario is considered herein, the helicopter transports the passengers from an assumed origin to a destination located 500km far from the origin. The engines operate at low power setting for 5 min prior and after the mission. Two H/C Take-Off Weight (TOW) cases are examined herein, one assuming TOW equal to 6000kg and one, more demanding, assuming TOW equal to 8000kg. Additionally, for each case a normal and a hot day (15ºC and 40ºC at Sea Level respectively) are considered. The mission flight and power profiles are depicted in Figure 10 and Figure 11 respectively.

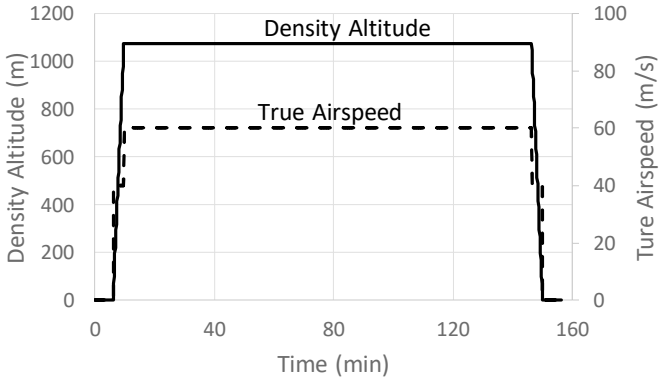

Figure 10: Mission density altitude and true airspeed flight profiles

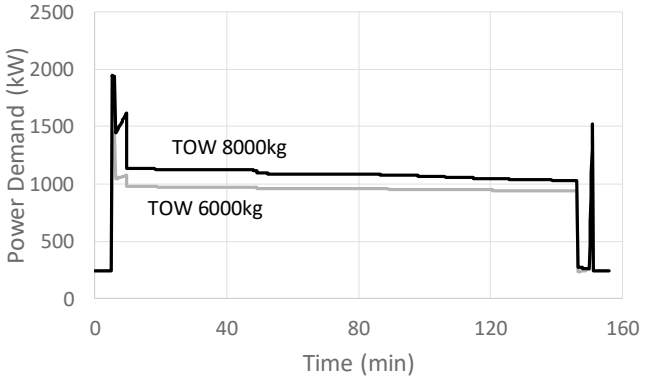

Figure 11: Mission total power requirement profile for TOW 6000kg and 8000kg

Baseline Power – Plant

The FOS temperatures and the cooling capacity for the conventional power plant (gas turbine) are calculated. Two cases are considered, one where the fuel is recirculating prior to the high-pressure pump (baseline FOS) and one where the fuel is recirculating to the tank. Figure 12 depicts the generated heat by the engine shaft bearings and the AGB for the test case mission for both TOW values. As seen, an increase in TOW increases the heat input as expected. The total mechanical losses related heat added to the system is in the range of 8 kW.

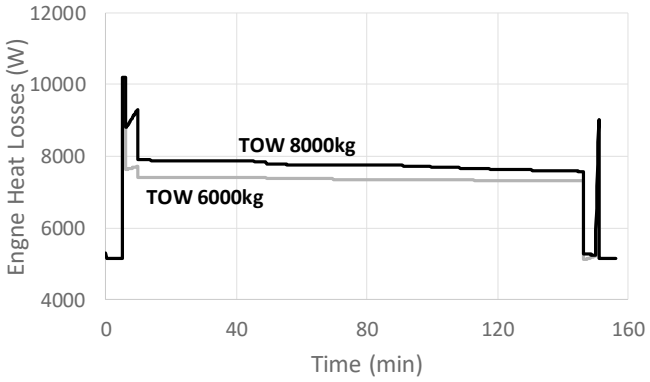

Figure 12: Heat load generated by the engine (AGB and bearings for TOW 6000kg and 8000kg

Baseline FOS

The fuel and oil temperatures of interest for TOW 6000kg and for a standard day of 15°C at Sea Level for the whole mission are depicted in Figure 13 and Figure 14**.** As seen for both sub-systems, the high temperatures in the mission are considerably lower compared

to the limiting values, highlighting that the FOS as designed herein has the potential to absorb more heat. In order to quantify this value, the cooling capacity of the baseline FOS over the mission is presented in Figure 15. The cooling capacity (CC) is defined as:

$$CC = W_f \cdot Cp_f \cdot \left(T_{limit} - T_{delivery}\right) \quad (8)$$

T_{limit} is selected as 130ºC with respect to Table 2 limits, $T_{delivery}$ is the combustor delivery temperature and W_f is the total fuel flow (recirculation and injection).

As seen, the fuel has a cooling capacity of approximately 15kW at the end of the mission. It is also interesting to identify that the worst operating point in terms of thermal absorption capability is descent, since fluids have already been heated and the fuel flow, which acts as heat sink, is reduced.

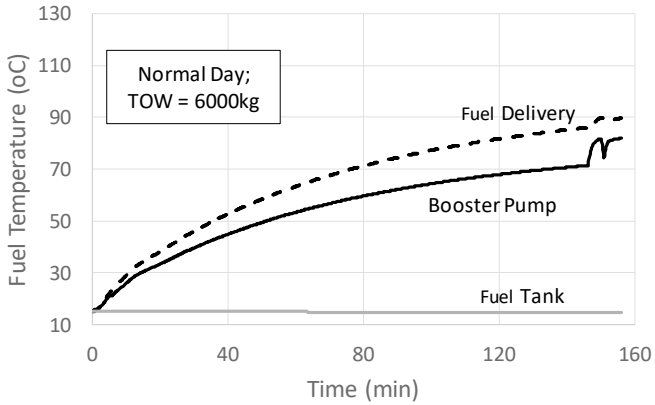

Figure 13: Fuel Temperature throughout the PAT mission

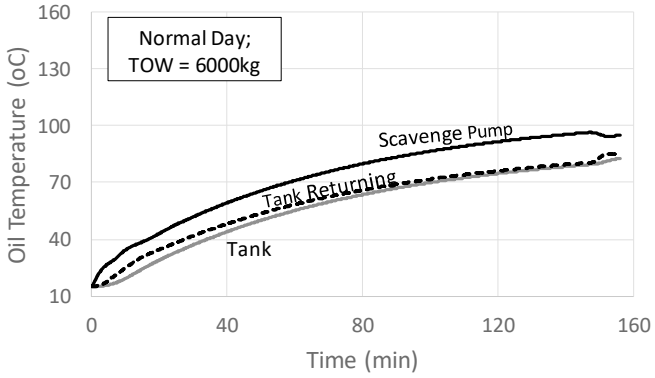

Figure 14: Oil Temperature throughout the PAT mission

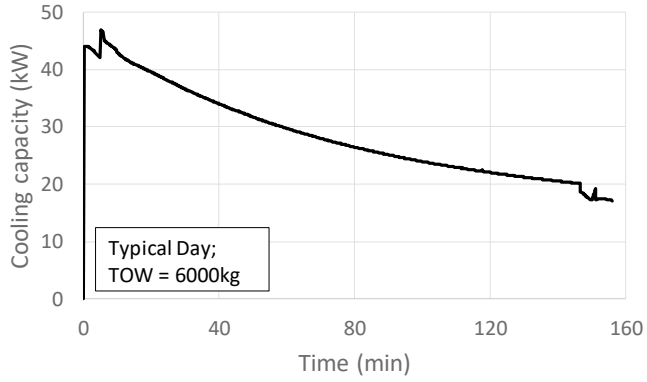

Figure 15: Fuel System cooling capacity throughout the PAT mission

The effect of TOW on the fuel and oil temperatures is depicted in Figure 16. For high values of TOW there is an increase of engine heat loads, but it is compensated by higher fuel flows. The scavenge pump and combustor fuel temperature are marginally increased for higher TOW values by 1 to 3 deg and at the final phase of the mission the temperature difference for the different TOW cases is negligible.

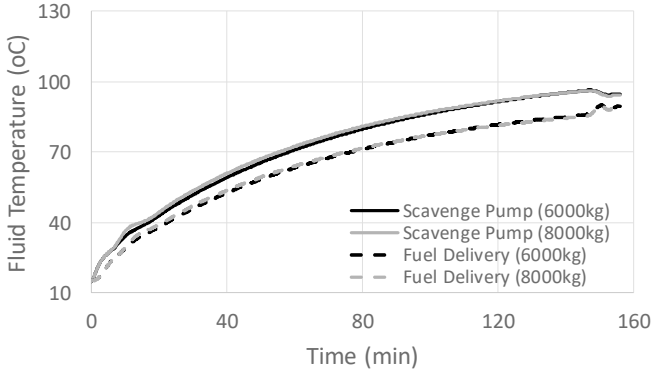

Figure 16: Subsystems high temperature for different TOW

For establishing the limits of the system, a hot day (40ºC at Sea Level) with TOW 8000kg is considered. As seen in Figure 17 the fuel temperature is approaching its limiting value for this case. At the end of the mission, there is a 20 deg margin. For the oil the temperature is higher compared to the baseline case but a margin of 30 deg still exists at the end of the mission (Figure 18). Concerning the cooling capacity, its final value is reduced from 15kW to 8.5kW, as seen in Figure 19.

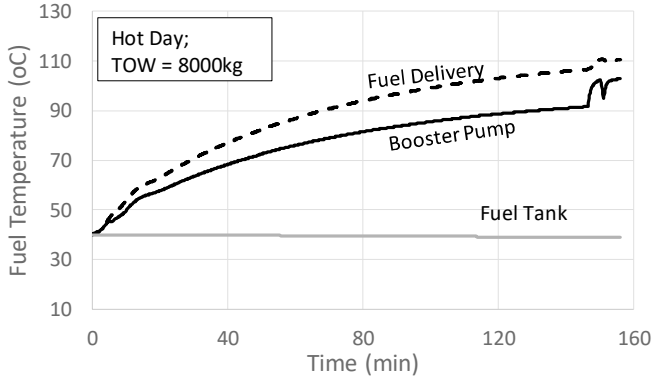

Figure 17: Fuel Temperature throughout the PAT mission for a hot day

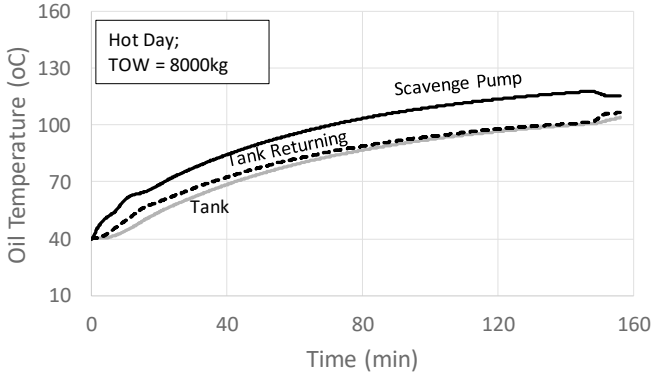

Figure 18:Oil Temperature throughout the PAT mission for a hot day

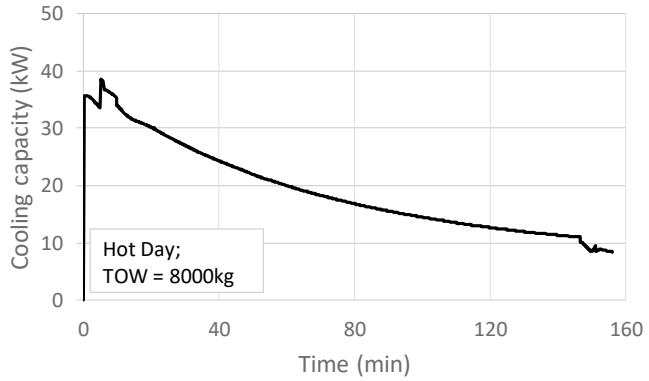

Figure 19: Fuel System cooling capacity throughout the PAT mission for a hot day

FOS with Fuel Recirculating at the Tank

If fuel tank recirculation is considered then the system heat capacity significantly increases, since the tank acts as a heat sink. In this case and for a hot day and TOW of 8000kg the fuel temperature margin at the end of the mission is in the range of 50 deg (Figure 20) and the cooling capacity is increased to approximately 20kW (Figure 21). It should be noted that for the tank recirculation case the fuel tank temperature is almost equal to the fuel pump temperature (boost pump).

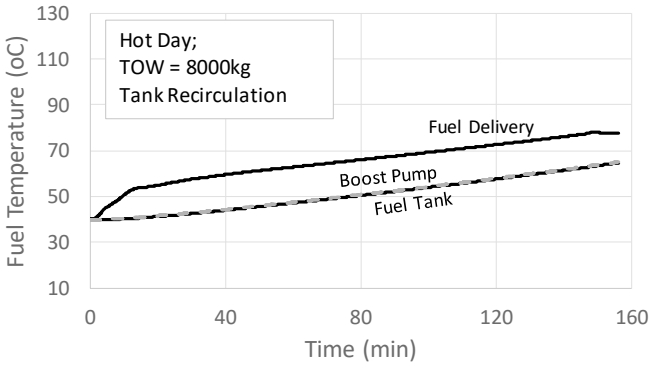

Figure 20: Fuel temperature throughout the PAT mission for a hot day and tank recirculation

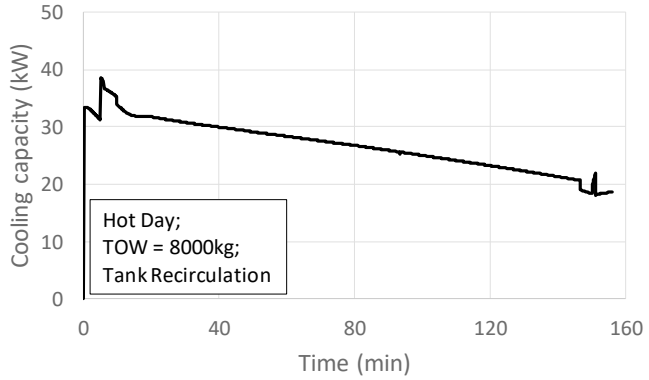

Figure 21: Fuel System cooling capacity throughout the PAT mission for a hot day and tank recirculation

It is interesting to note that increasing the tank fuel temperature enhances the atmosphere – tank walls heat transfer, hence in this case atmosphere is becoming a heat sink as well. The tank-atmosphere maximum heat transferred through the mission is in the range of 400W and occurs during descent. Despite the benefits of using the fuel tank as a heat sink, the increase of the tank temperature and consequently of the fuel vapour temperature may give rise to flammability issues and this should be further assessed.

Thermo-Electric Power – Plant

Three main PMS cases are considered herein, one which is considered as the worst case and two with varying hybridization level. For each PMS case the motor, controller and battery are redesigned. Specifically, the electric power train (motor, controller, and battery) is sized based on nominal power, energy and voltage. For establishing the system limits a TOW of 8000kg for a hot day of 40ºC is considered.

The first PMS (PMS1) applied is utilizing the electric power train for providing all the power during Take Off (T/O), climb and descent. The gas turbine is idling during these phases and provides power during cruise. The electric power train (motor, controller, and battery) is sized based on the maximum continuous power of the engine (987kW) and the energy demand for the first two phases (T/O and climb) (80kWh), while the voltage is considered 3000V as suggested in [41]. The battery is recharged during cruise. PMS1 is considered the worst test case from a thermal management point of view since all power is provided by the electric power train; hence, the heat produced is the maximum possible during normal operation, and the fuel flow, which acts as heat sink, has its lower value. Additionally it is a case of interest since it may be a way to avoid brownout effect on engine reducing its deterioration [3].

Next and in order to examine the hybridization effect on the FOS capability to act as a heat sink, two cases of different hybridization degree are considered. As discussed by the authors [5] for current technology level and TEM rotorcraft propulsion low degree of hybridization should be considered. In this context the second PMS (PMS2) assessed herein is 10% hybrid (160kW, 200kWh) and the third (PMS3) 20% hybrid (240kW, 340kWh), assuming a nominal voltage of 580V for both cases, as suggested in [41]. As depicted in Figure 9 the electric power train heat is added to the system after the fuel – oil heat exchanger (FOH).

Power Management Strategy 1

In the case of PMS1 high thermal power is produced and has to be treated in a short period, as seen in Figure 22. It is apparent that the baseline and the recirculated FOS system can not cope with this heat production, since fuel cooling capacity at the mission start is less than 40kW. This is confirmed by the fuel temperature value for the tank recirculating FOS seen in Figure 23.

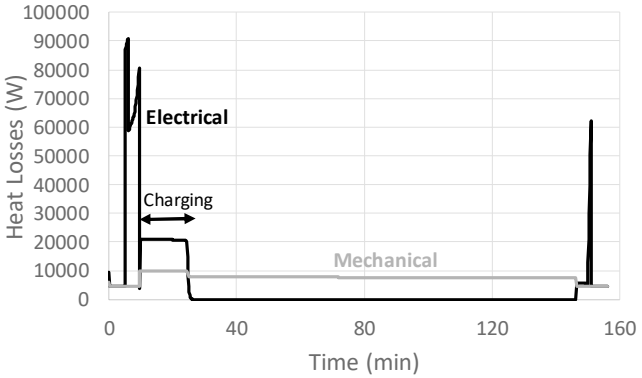

Figure 22: Heat load generated by the propulsion system for TOW 8000kg – PMS1

The high temperature is due to the high heat input during the mission initial phase, while the total heat energy added during the whole mission is not having a significant effect on the final temperature. A method to assess this problem is to maximize the recirculating fuel flow during this critical phase. As seen in Figure 24 the maximum fuel temperature is reduced by approximately 20deg to 160ºC, which is higher than the fuel temperature limit. Based on this, resizing the flows, the piping and the heat exchangers may be a way to further enhance the cooling capacity of the baseline FOS, but aspects such as weight, auxiliary power consumption and cost increase should be considered versus other options such as adding another heat sink (e.g. air). In case that the battery is not recharging the final temperature is lower but still fuel temperature overshoots at the first phase.

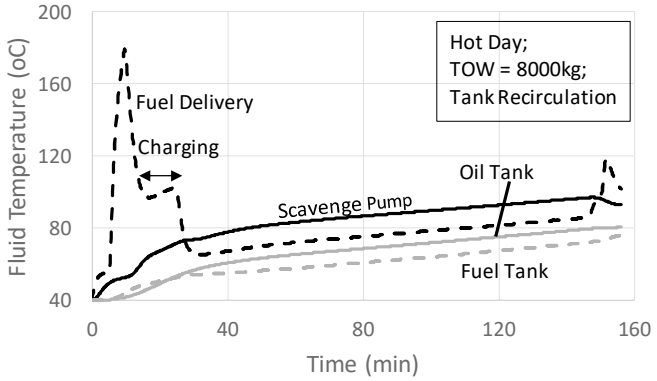

Figure 23: Fuel delivery, oil scavenge pump and tank temperatures for a hot day and tank recirculation, PMS1

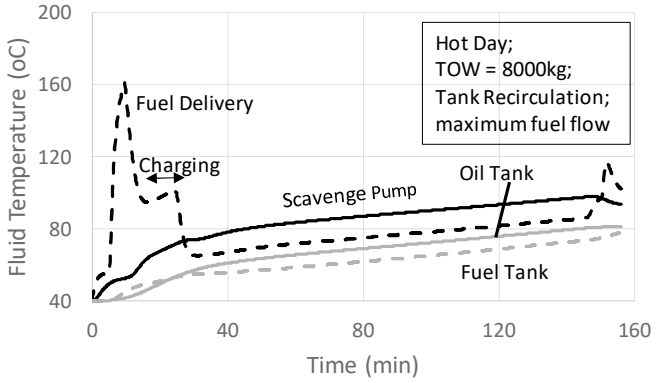

Figure 24: Fuel delivery, oil scavenge pump and tank temperatures for a hot day, tank recirculation and maximum fuel flow during T/O and climb, PMS1

Power Management Strategy 2

PMS2 is a low hybridization case, where the electric power train provide 10% of the propulsion power needed. The heat, that has to be treated, produced by the propulsion system is depicted in Figure 25. In this case, the critical parameter is the thermal energy that has to be treated by the FOS.

As seen in Figure 26 the baseline FOS can to some extent treat the heat, and fuel reaches its maximum allowable temperature at the end of the mission. These results indicate that applying an active fuel flow control may be a suitable way to address heat loads without system changes for this case. Recirculation to tank FOS is rather effective for this degree of hybridization, as seen in Figure 27. All temperatures are lower than the considered limits.

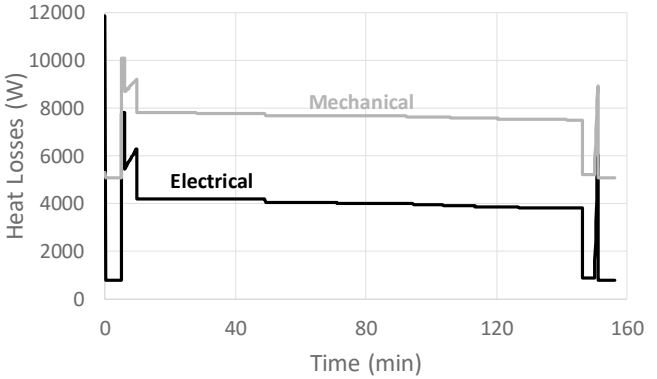

Figure 25: Heat load generated by the propulsion system for TOW 8000kg for PMS2

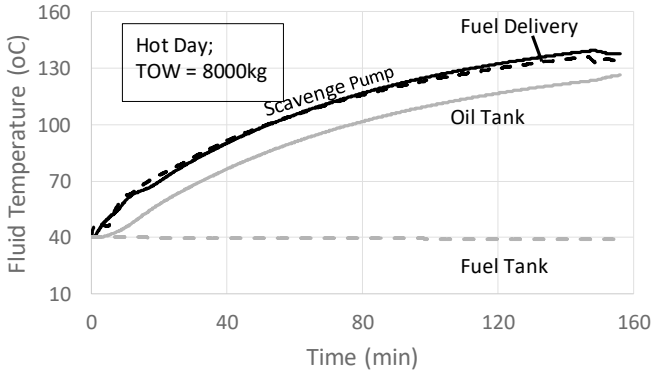

Figure 26: Fuel delivery, oil scavenge pump and tank temperatures for a hot day, PMS2

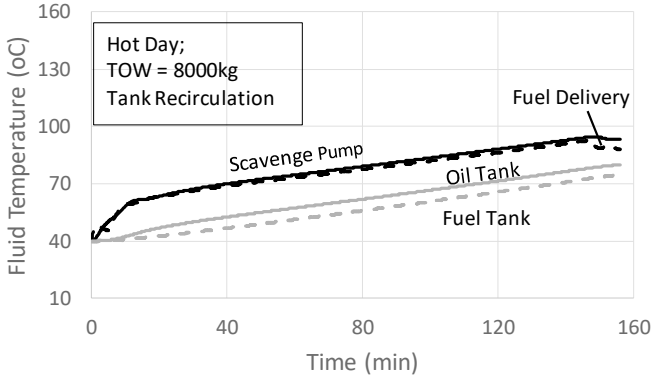

Figure 27: Fuel delivery, oil scavenge pump and tank temperatures for a hot day and tank recirculation, PMS2

Power Management Strategy 3

For the case of PMS3 the electric power train provides 20% of the propulsion power needed. The heat produced by the propulsion system, that has to be treated, is depicted in Figure 28.

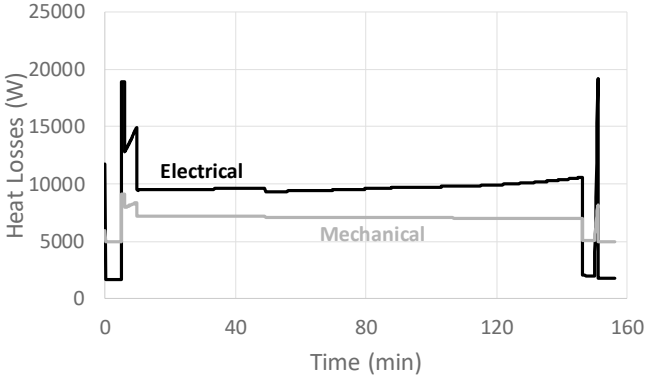

Figure 28: Heat load generated by the propulsion system for TOW 8000kg for PMS3

In this case, the critical parameter is again the thermal energy that has to be treated by the FOS. For the baseline FOS configuration the recirculating fuel flow throughout the mission is the maximum one for enhancing cooling capacity of the system. As seen in Figure 29 even when the maximum recirculating fuel flow is considered the fuel and oil temperatures exceeds the limits. For the case of tank recirculation, the tank has enough thermal inertia to dissipate the propulsion system thermal loads, as demonstrated in Figure 30.

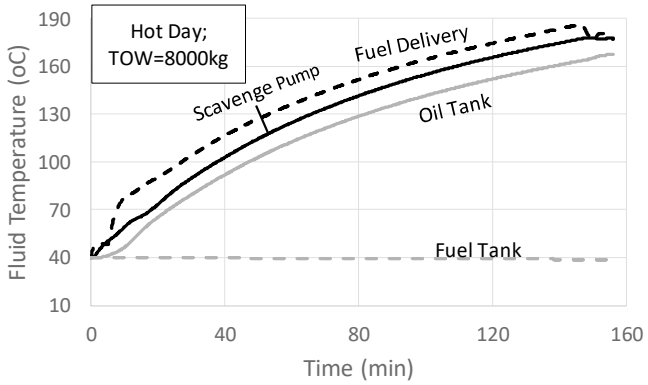

Figure 29: Fuel delivery, oil scavenge pump and tank temperatures for a hot day, PMS3

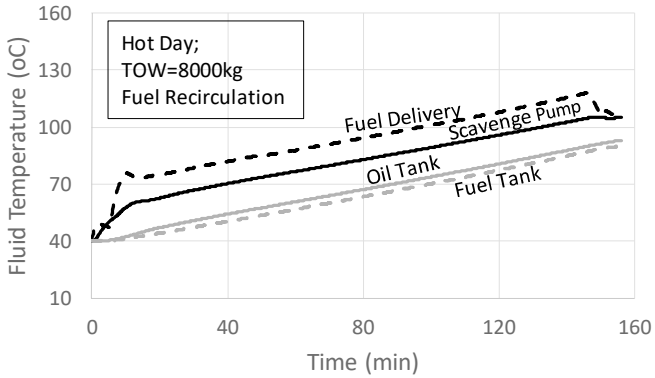

Figure 30: Fuel delivery, oil scavenge pump and tank temperatures for a hot day and tank recirculation, PMS3

SUMMARY AND CONCLUSION

An integrated thermal management and propulsion system model is developed for assessing the cooling capacity of FOS for future hybrid electric rotorcraft configurations. The simulation model integrates a gas turbine, an electric power train, and a representative fuel and oil system using Simcenter Amesim. The developed model is capable to simulate different helicopter missions, calculating propulsion system and FOS performance and operational data. A representative rotorcraft Passenger Air Transport (PAT) mission is analyzed. Two FOS configurations are examined, the baseline one and one where fuel tank recirculation is applied for enhancing system cooling capacity. Three different PMS are considered. The first, which is rather demanding in terms of thermal loads, is utilizing the electric power train for providing power during T/O, climb and descent and the gas turbine during cruise. The next two PMS assess different level of hybridization (10% and 20%).

In terms of fuel system cooling capacity, the descent phase seems to be the critical one, hence it is the phase that should be considered when high electrical energy missions are assessed. For hybrid electric propulsion, the results suggest that the baseline FOS will not be able to tackle the electric heat loads for cases of degree of hybridization more than 10%. Specifically if maximum recirculation flow is applied then the baseline FOS can cope with the heat loads for degree of hybridization up to 10%. This result indicates that an active controllable boost pump for controlling the recirculating flow is a promising strategy for ensuring safe operation.

For higher degree of hybridization, in the range of 20%, the baseline FOS is not an option. A variation of the baseline FOS with fuel recirculating to the tank can provide additional cooling capacity. This configuration can successfully act as a thermal management system for the 20% degree of hybridization. In the case of exploiting the heat capacity of the fuel tank with recirculating flow, the fuel vapour flammability should be examined and fuel tank inerting may be necessary.

The utilization of electric power during T/O is not an option for the power range and electric components efficiency examined herein. Even when recirculating the maximum flow to the fuel tank, the fuel delivery temperature exceeds significantly (by approximately 30 deg) the steady state limiting fuel temperature. In this case, an additional heat sink should be considered.

REFERENCES

[1] Airbus, 2016, “Global Market Forecast, Mapping Demand 2016/2035," Technical report

[2] Report of the High Level Group on Aviation Research, 2011, “Flightpath 2050, Europe’s Vision for Aviation Maintaining Global Leadership & Serving Society’s Needs”, Directorate-General for Research and Innovation Directorate-General for Mobility and Transport

[3] Danis R. A., Green M. W., Freeman J. L, Hall D.W., 2018, “Examining the Conceptual Design Process for Future Hybrid-Electric Rotorcraft”, NASA/CR—2018–219897
[4] Voskuijl, M., van Bogaert, J. and Rao, A. G., 2017, “Analysis and Design of Hybrid Electric Regional Turboprop Aircraft”, CEAS Aeronautical Journal. Springer Vienna, 9(1), pp. 15–25
[5] Roumeliotis I., Mourouzidis C., Zaffereti M., Pachidis V., Broca O., Unlu D., 2019, “Assessment of Thermo-Electric Power Plants for Rotorcraft Application”, ASME paper No. GT2019-91481
[6] Kirner R., Raffaelli L., Rolt A., Laskaridis P., Doulgeris G. & Singh R., 2015, “An assessment of distributed propulsion: Advanced propulsion system architectures for conventional aircraft configurations”, Aerospace Science and Technology, 46 42-50
[7] Jafari, S.; Nikolaidis, T., 2018, “Thermal Management Systems for Civil Aircraft Engines: Review, Challenges and Exploring the Future”, Appl. Sci. 2018, 8, 2044
[8] Benjamin J. Brelje, Joaquim R.R.A. Martins, 2019, “Electric, hybrid, and turboelectric fixed-wing aircraft: A review of concepts, models, and design approaches”, Progress in Aerospace Sciences, Volume 104, 2019, Pages 1-19
[9] Yitao Liu, Y.; Deng, J.; Liu, C.; Li, S., 2018, “Energy optimization analysis of the more electric aircraft”, IOP Conf. Series: Earth and Environmental Science 113 (2018) 012152
[10] Yanqing Li, Yimin Xuan, 2019, “Integrated Thermal Modeling of Helicopters”, Applied Thermal Engineering”, Volume 154, 2019, Pages 458-468
[11] Wolff, M., 2011, “Aerothermal Design of an Engine/Vehicle Thermal Management System,” Tech. Rep. RTO-EN-AVT-195, North Atlantic Treaty Organization
[12] Walters E. A., Iden S. et al., 2010, “INVENT modeling, simulation, analysis and optimization,” in Proceedings of the 48th AIAA Aerospace Sciences Meeting Including the New Horizons Forum and Aerospace Exposition, Orlando, Fla, USA, January 2010
[13]”Siemens PLM Software Simcenter”
https://www.plm.automation.siemens.com/global/en/products/simcenter/
[14] Greenwood, E., Schmitz, F. H., & Sickenberger, R. D., 2015, “A semiempirical noise modeling method for helicopter maneuvering flight operations”. Journal of the American Helicopter Society, 60(2), 1-13
[15] Leishman, G. J., 2006, “Principles of Helicopter Aerodynamics with CD Extra”. Cambridge University press
[16] Hilbert, K. B., 1984, “A mathematical model of the UH-60 helicopter”. NASA TM 85890.
[17] Yeo, H., Bousman, W. G., & Johnson, W., 2004, “Performance Analysis of a Utility Helicopter with Standard and Advanced Rotors”. Journal of the American Helicopter Society, 49(3), 250-270
[18] Hu, X., Jiang, Y., Luo, C., Feng, L. and Dai, Y., 2019. “Churning Power Losses of A Gearbox with Spiral Bevel Geared Transmission”, Tribology International, 129, pp.398-406
[19] Fernandes, C.M.D.C.G., 2015, “Power Loss in Rolling Bearings and Gears Lubricated with Wind Turbine Gear Oils”, PhD thesis, submitted in Universidade Do Porto
[20] Changenet, C., Leprince, G., Ville, F. and Velex, P., 2011, “A Note on Flow Regimes and Churning Loss Modeling”, Journal of Mechanical Design, 133(12), p.121009
[21] Buckingham, E., 1949, “Analytical Mechanics of Gears”, McGraw-Hill Book Co
[22] Terekhov, A.S., 1975, “Hydraulic Losses in Gearboxes with Oil Immersion”, Russian Engineering Journal, 55(5), pp.7-11.
[23] Ohlendorf, H, 1958, “Verlustleistung und Erwärmung von Stirnrädern”, Doctoral dissertation, Technische Universität München
[24] Gao W., Lyu Y., Liu Z., Nelias D., “Validation and application of a numerical approach for the estimation of drag and churning losses in high speed roller bearings”, Applied Thermal Engineering, Volume 153, 2019, Pages 390-397
[25] Freudenberg Simrit GmbH & Co., 1976, “Radialwellendichtringe, Katalog Nr. 100”
[26] Fernandes, C.M., Marques, P.M., Martins, R.C., Seabra, J.H., 2015, “Gearbox Power Loss. Part III: Application To a Parallel Axis and a Planetary Gearbox” Tribology International, 88, pp.317-326.
[27] Gaudet S.R, Gauthier J. E. D., 2007, “A Simple Sub-Idle Component Map Extrapolation Method”, ASME paper No GT2007-27193.
[28] Ballin M. G., 1988, “A High Fidelity Real-Time Simulation of a Small Turboshaft Engine”, Technical report, NASA Ames Research Center
[29] Frosina, E., Senatore, A., Palumbo, L., Di Lorenzo, G., Pascarella, C., 2018, “Development of a Lumped Parameter Model for an Aeronautic Hybrid Electric Propulsion System”, Aerospace 2018, 5(4), 105
[30] Hangiu Radu-Petru, Filip Andrei-Toader, Martis Claudia Steluta, Biró Károly Ágoston, 2012, “System-level Modeling and Simulation of a Permanent Magnet Synchronous Motor for an Integrated Starter Alternator”. Journal of Electrical and Electronics Engineering, 5(2):67-70
[31] Vratny C. P., Forsbach F., Seitz A., Hornung M., 2014, “Investigation of Universally Electric Propulsion Systems for Transport Aircraft”, 29th Congress of the International Council of the Aeronautical Sciences at: St. Petersburg, Russia
[32] Robert A. McDonald. "Electric Propulsion Modeling for Conceptual Aircraft Design", 52nd Aerospace Sciences Meeting, AIAA SciTech Forum, (AIAA 2014-0536)

[33] Wintrich A., Nicolai U., Tursky W., Reimann T., 2015, “Power Semiconductors”, Semikron, Semikron International GmBh, Verlag, 2015
[34] Nicolas Marc. Méthodologie de dimensionnement d'un véhicule hybride électrique sous contrainte de minimisation des émissions de CO2. Université d'Orléans, 2013
[35] M. Petit, N. Marc, F. Badin, R. Mingant and V. Sauvant-Moynot, A Tool for Vehicle Electrical Storage System Sizing and Modelling for System Simulation, 2014 IEEE Vehicle Power and Propulsion Conference (VPPC), Coimbra, p. 91-96
[36] Bearing calculation Extract from the Railway technical handbook, volume 1, chapter 5, page 106 to 121, https://www.skf.com/binary/49-62749/RTB-1-05-Bearing-calculation.pdf
[37] The SKF model for calculating the frictional moment, https://www.skf.com/binary/12-299767/0901d1968065e9e7-The-SKF-model-for-calculating-the-frictional-movement_tcm_12-299767.pdf
[38] CATERPILAR, 1998, Marine Engine Application and Installation Guide, Diesel Engine Systems – Piping,
[39] R. Shawabkeh, “Steps for design of Heat Exchanger”, http://elearning.utm.my/17182/pluginfile.php/322751/mod_resource/content/1/Design_of_Heat_Exchanger.pdf
[40] Streifinger, H., 1998, “Fuel/Oil System Thermal Management in Aircraft Turbine Engines”, NATO RTO Symposium, Design principles and methods for aircraft gas turbine engines; 1998; Toulouse; France
[41] Anton F., 2019, “eAircraft: Hybrid-elektrische Antriebe für Luftfahrzeuge”, Siemens AG, Corporate Technology14. Tag der Deutschen Luft-und-Raumfahrtregionen, Potsdam, 10. September2019